



ELSEVIER

12 November 1998

PHYSICS LETTERS B

Physics Letters B 440 (1998) 225–232

A measurement of the branching fractions  
of the  $f_1(1285)$  and  $f_1(1420)$   
produced in central pp interactions at 450 GeV/c

WA102 Collaboration

D. Barberis <sup>d</sup>, W. Beusch <sup>d</sup>, F.G. Binon <sup>f</sup>, A.M. Blick <sup>e</sup>, F.E. Close <sup>c,d</sup>,  
K.M. Danielsen <sup>k</sup>, A.V. Dolgoplov <sup>e</sup>, S.V. Donskov <sup>e</sup>, B.C. Earl <sup>c</sup>, D. Evans <sup>c</sup>,  
B.R. French <sup>d</sup>, T. Hino <sup>l</sup>, S. Inaba <sup>h</sup>, A.V. Inyakin <sup>e</sup>, T. Ishida <sup>h</sup>, A. Jacholkowski <sup>d</sup>,  
T. Jacobsen <sup>k</sup>, G.T Jones <sup>c</sup>, G.V. Khaustov <sup>e</sup>, T. Kinashi <sup>m</sup>, J.B. Kinson <sup>c</sup>, A. Kirk <sup>c</sup>,  
W. Klempt <sup>d</sup>, V. Kolosov <sup>e</sup>, A.A. Kondashov <sup>e</sup>, A.A. Lednev <sup>e</sup>, V. Lenti <sup>d</sup>,  
S. Maljukov <sup>g</sup>, P. Martinengo <sup>d</sup>, I. Minashvili <sup>g</sup>, T. Nakagawa <sup>l</sup>, K.L. Norman <sup>c</sup>,  
J.P. Peigneux <sup>a</sup>, S.A. Polovnikov <sup>e</sup>, V.A. Polyakov <sup>e</sup>, V. Romanovsky <sup>g</sup>,  
H. Rotscheidt <sup>d</sup>, V. Rumyantsev <sup>g</sup>, N. Russakovich <sup>g</sup>, V.D. Samoylenko <sup>e</sup>,  
A. Semenov <sup>g</sup>, M. Sené <sup>d</sup>, R. Sené <sup>d</sup>, P.M. Shagin <sup>e</sup>, H. Shimizu <sup>m</sup>,  
A.V. Singovsky <sup>a,e</sup>, A. Sobol <sup>e</sup>, A. Solovjev <sup>g</sup>, M. Stassinaki <sup>b</sup>, J.P. Stroot <sup>f</sup>,  
V.P. Sugonyaev <sup>e</sup>, K. Takamatsu <sup>i</sup>, G. Tchlatchidze <sup>g</sup>, T. Tsuru <sup>h</sup>, M. Venables <sup>c</sup>,  
O. Villalobos Baillie <sup>c</sup>, M.F. Votruba <sup>c</sup>, Y. Yasu <sup>h</sup>

<sup>a</sup> LAPP-IN2P3, Annecy, France

<sup>b</sup> Athens University, Physics Department, Athens, Greece

<sup>c</sup> School of Physics and Astronomy, University of Birmingham, Birmingham, UK

<sup>d</sup> CERN - European Organization for Nuclear Research, Geneva, Switzerland

<sup>e</sup> IHEP, Protvino, Russia

<sup>f</sup> IISN, Belgium

<sup>g</sup> JINR, Dubna, Russia

<sup>h</sup> High Energy Accelerator Research Organization (KEK), Tsukuba, Ibaraki 305, Japan

<sup>i</sup> Faculty of Engineering, Miyazaki University, Miyazaki, Japan

<sup>j</sup> RCNP, Osaka University, Osaka, Japan

<sup>k</sup> Oslo University, Oslo, Norway

<sup>l</sup> Faculty of Science, Tohoku University, Aoba-ku, Sendai 980, Japan

<sup>m</sup> Faculty of Science, Yamagata University, Yamagata 990, Japan

Received 22 September 1998; revised 30 September 1998

Editor: L. Montanet

## Abstract

A study of the  $f_1(1285)$  and  $f_1(1420)$  produced in central pp interactions has been performed. For the first time in a single experiment the branching fractions of both mesons in all major decay modes have been determined. Both the  $f_1(1285)$  and  $f_1(1420)$  are consistent with being produced by double Pomeron exchange. © 1998 Elsevier Science B.V. All rights reserved.

In central production the  $J^{PC} = 1^{++}$   $f_1(1285)$  and  $f_1(1420)$  are clearly observed [1,2]. In contrast, there is no evidence for any  $0^{-+}$  contribution in the 1.28 and 1.4 GeV regions [1–3]. This suppression of  $0^{-+}$  states in central production was first observed by experiment WA76 at the CERN Omega Spectrometer [1] and has been independently confirmed by the E690 experiment at Fermilab [4]. Although the reason for this suppression of  $0^{-+}$  states is not known it has a very important implication since it can help us determine more precisely the characteristics of the  $f_1(1285)$  and  $f_1(1420)$  than is possible in other experiments which see both  $0^{-+}$  and  $1^{++}$  states.

Experiment WA102 is designed to study centrally produced exclusive final states formed in the reaction

$$pp \rightarrow p_f(X^0)p_s \quad (1)$$

at 450 GeV/c. The subscripts  $f$  and  $s$  indicate the fastest and slowest particles in the laboratory respectively and  $X^0$  represents the central system that is presumed to be produced by double exchange processes. The experiment has been performed using the CERN Omega Spectrometer, the layout of which is described in Ref. [5].

Analyses of the  $K_S^0 K^\pm \pi^\mp$  and  $\pi^+ \pi^- \pi^+ \pi^-$  channels have been published previously [6,7]. This paper presents a study of the  $f_1(1285)$  and  $f_1(1420)$  through an analysis of the  $\eta \pi^+ \pi^-$ ,  $\rho^0 \gamma$  and  $\phi \gamma$  channels.

The reaction

$$pp \rightarrow p_f(\eta \pi^+ \pi^-) p_s \quad (2)$$

where the  $\eta$  has been observed decaying to  $\gamma \gamma$  and  $\pi^+ \pi^- \pi^0$ , has been isolated from the sample of events having four and six outgoing charged tracks respectively plus two  $\gamma$ s each with energy greater

than 0.5 GeV reconstructed in the electromagnetic calorimeter<sup>1</sup>, by first imposing the following cuts on the components of the missing momentum:  $|\text{missing } P_x| < 17.0 \text{ GeV}/c$ ,  $|\text{missing } P_y| < 0.16 \text{ GeV}/c$  and  $|\text{missing } P_z| < 0.12 \text{ GeV}/c$ , where the  $x$ -axis is along the beam direction. A correlation between pulse-height and momentum obtained from a system of scintillation counters was used to ensure that the slow particle was a proton.

For the case  $\eta \rightarrow \gamma \gamma$  the effective mass of the two  $\gamma$ s is shown in Fig. 1(a) for the events contributing to the  $f_1(1285)$  mass region of the  $\eta \pi^+ \pi^-$  spectrum. The  $\gamma \gamma$  mass spectrum shows a clear  $\eta$  signal ( $\sigma = 31 \text{ MeV}$ ) with little background, which was selected by requiring  $0.45 < m(\gamma \gamma) < 0.65 \text{ GeV}$ . For the case  $\eta \rightarrow \pi^+ \pi^- \pi^0$  the effective mass of the  $\pi^+ \pi^- \pi^0$  is shown in Fig. 1(b) for the events contributing to the  $f_1(1285)$  mass region of the  $\eta \pi^+ \pi^-$  spectrum. The  $\pi^+ \pi^- \pi^0$  mass spectrum shows a clear  $\eta$  signal ( $\sigma = 11 \text{ MeV}$ ) with effectively no background, which was selected by requiring  $0.5 < m(\pi^+ \pi^- \pi^0) < 0.6 \text{ GeV}$ . The quantity  $\Delta$ , defined as  $\Delta = MM^2(p_f p_s) - M^2(\eta \pi^+ \pi^-)$ , where  $MM^2(p_f p_s)$  is the missing mass squared of the two outgoing protons, was then calculated for each event and a cut of  $|\Delta| \leq 3.0 \text{ GeV}^2$  was used to select the  $\eta \pi^+ \pi^-$  channel. Events containing a fast  $\Delta^{++}(1232)$  were removed if  $M(p_f p_s) < 1.3 \text{ GeV}$ , which left 90 393 centrally produced  $\eta \pi^+ \pi^-$  events for  $\eta \rightarrow \gamma \gamma$  and 24 585 for  $\eta \rightarrow \pi^+ \pi^- \pi^0$ . After the selection of the  $\eta \pi^+ \pi^-$  channel a kinematical fit was performed in order to apply overall energy and momentum balance.

<sup>1</sup> The showers associated with the impact of the charged tracks on the calorimeter have been removed from the event before the requirement of only two  $\gamma$ s was made.

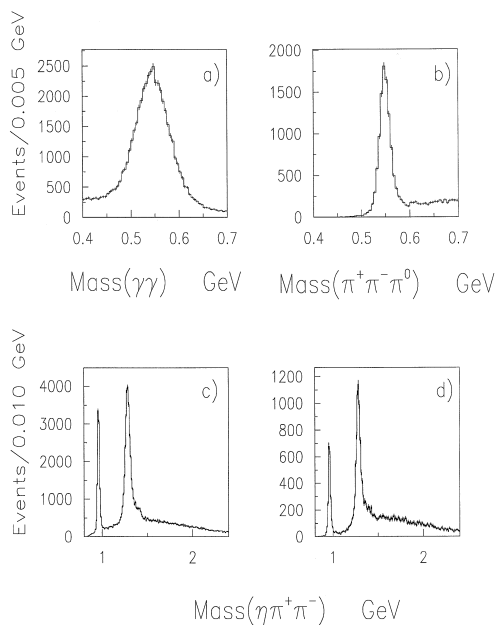


Fig. 1. (a) The  $\gamma\gamma$  mass spectrum and (b) the  $\pi^+\pi^-\pi^0$  mass spectrum contributing to the  $f_1(1285)$  mass region of the  $\eta\pi^+\pi^-$  spectrum. The  $\eta\pi^+\pi^-$  mass spectrum for (c)  $\eta \rightarrow \gamma\gamma$  and (d)  $\eta \rightarrow \pi^+\pi^-\pi^0$ .

Fig. 1(c) and (d) shows the  $\eta\pi^+\pi^-$  effective mass spectrum for  $\eta \rightarrow \gamma\gamma$  and  $\eta \rightarrow \pi^+\pi^-\pi^0$  respectively. Clear peaks of the  $\eta'$  and  $f_1(1285)$  can be seen together with a shoulder in the 1.4 GeV mass region. A fit to these spectra has been attempted using a Gaussian to describe the  $\eta'$ , a Breit-Wigner convoluted with a Gaussian, to account for the experimental resolution ( $\sigma = 21$  MeV for  $\eta \rightarrow \gamma\gamma$  and  $\sigma = 17$  MeV for  $\eta \rightarrow \pi^+\pi^-\pi^0$ ), to describe the  $f_1(1285)$  and a background of the form  $a(m - m_{\text{th}})^b \exp(-cm - dm^2)$ , where  $m$  is the  $\eta\pi^+\pi^-$  mass,  $m_{\text{th}}$  is the threshold mass and  $a, b, c, d$  are fit parameters. The fit (not shown) fails to describe the 1.4 GeV region. Fig. 2(a) shows the result of the fit (for the case  $\eta \rightarrow \gamma\gamma$ ) including a Breit-Wigner to describe the 1.4 GeV region which yields a mass of  $1370 \pm 5$  MeV and a width of  $109 \pm 18$  MeV. We did not observe anything in this mass region in the analysis of the  $K_S^0 K^\pm \pi^\mp$  channel [6] and these parameters are lower in mass and broader in width than states observed in the  $\eta\pi^+\pi^-$  channel by other experiments [8]. This may suggest that the shoulder

is due to an interference effect and this possibility will be discussed below.

A spin-parity analysis of the  $\eta\pi^+\pi^-$  channel has been performed in the mass interval 1.2 to 1.5 GeV using an isobar model [9]. Assuming that only angular momenta up to 2 contribute, the intermediate states considered are  $a_0(980)\pi$  and  $\sigma\eta$ , where  $\sigma$  stands for the low mass  $\pi\pi$  S-wave amplitude squared [10]. The amplitudes have been calculated in the spin-orbit (LS) scheme using spherical harmonics. In order to perform a spin parity analysis the log likelihood function,  $\mathcal{L}_j = \sum_i \log P_j(i)$ , is defined by combining the probabilities of all events in 20 MeV  $\eta\pi^+\pi^-$  mass bins from 1.2 to 1.5 GeV. The incoherent sum of various event fractions  $a_j$  is calculated so as to include more than one wave in the fit,

$$\mathcal{L} = \sum_i \log \left( \sum_j a_j P_j(i) + \left( 1 - \sum_j a_j \right) \right) \quad (3)$$

where the term  $(1 - \sum_j a_j)$  represents the phase space background. The negative log likelihood function ( $-\mathcal{L}$ ) is then minimised using MINUIT [11]. Different combinations of waves and isobars have been tried and insignificant contributions have been removed from the final fit.

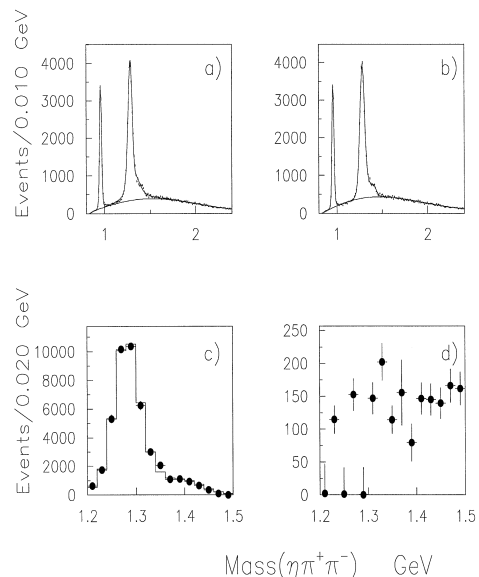


Fig. 2. (a) and (b) the  $\eta\pi^+\pi^-$  mass spectrum with fits described in the text. (c) The  $J^{PC} = 1^{++}$   $a_0(980)\pi$  wave and (d) the  $J^{PC} = 0^{-+}$   $a_0(980)\pi$  wave.

The only wave required in the fit is the  $J^{PC} = 1^{++}$   $a_0(980)\pi$  wave with spin projection  $|J_z| = 1$ . No  $J^{PC} = 0^{-+}$   $a_0(980)\pi$  or any  $\sigma\eta$  waves are required in the fit. Fig. 2(c) shows the  $J^{PC} = 1^{++}$   $a_0(980)\pi$  wave where the  $f_1(1285)$  and the shoulder at 1.4 GeV can be seen. Even though the addition of the  $J^{PC} = 0^{-+}$   $a_0(980)\pi$  wave makes an insignificant change to the likelihood we have included it and show the result in Fig. 2(d) where a flat distribution can be observed.

The fact that the shoulder at 1.4 GeV appears in the  $J^{PC} = 1^{++}$   $a_0(980)\pi$  wave suggests that it could be due to the  $f_1(1420)$ . However, the mass obtained using two incoherent Breit-Wigners, as described above, did not give mass and width parameters compatible with the  $f_1(1420)$ . If the  $f_1(1420)$  did have an  $a_0(980)\pi$  decay mode then a possible solution is that, since both the  $f_1(1285)$  and  $f_1(1420)$  have the same quantum numbers and decay mode, they could interfere.

In order to test the interference hypothesis a fit has been performed to the  $\eta\pi^+\pi^-$  mass spectrum (shown in Fig. 2(b)) and to the  $J^{PC} = 1^{++}$   $a_0(980)\pi$  wave in Fig. 2(c) using a K matrix formalism [12] including poles to describe the interference between the  $f_1(1285)$  and the  $f_1(1420)$ . The parameters of the poles have been fixed to the values obtained for the  $f_1(1285)$  and the  $f_1(1420)$  from a fit to the  $K_S^0 K^\pm \pi^\mp$  mass spectrum [6] and the resulting function smeared to take into account the experimental resolution. The only free parameters are the relative phase between the resonances and their relative production strengths. As can be seen from Fig. 2(b) and c) the parameterisation describes well both the total mass spectrum and the  $J^{PC} = 1^{++}$   $a_0(980)\pi$  wave. The relative phase is found to be  $154 \pm 9$  degrees. Therefore, the shoulder at 1.4 GeV can be interpreted as an  $a_0(980)\pi$  decay mode of the  $f_1(1420)$ .

In order to determine the branching ratio of the  $f_1(1285)$  and the  $f_1(1420)$  a number of checks have been employed. Firstly, we have measured the acceptance corrected number of  $\eta'$  and  $f_1(1285)$  observed in the  $\eta\pi^+\pi^-$  mass spectrum for the cases where the  $\eta$  decays to  $\gamma\gamma$  and  $\pi^+\pi^-\pi^0$  and hence have determined the  $\eta$  branching ratio to be

$$\frac{\eta \rightarrow \gamma\gamma}{\eta \rightarrow \pi^+\pi^-\pi^0} = 1.70 \pm 0.09 \pm 0.02 \quad (4)$$

which is in good agreement with the PDG value of  $1.70 \pm 0.04$  [8].

We have previously measured the  $f_1(1285)$  branching ratio in the  $\pi^+\pi^-\pi^+\pi^-$  and  $K_S^0 K^\pm \pi^\mp$  channels. Here we compare the  $\eta\pi\pi$  to the  $K\bar{K}\pi$  for which we determine

$$\frac{f_1(1285) \rightarrow K\bar{K}\pi}{f_1(1285) \rightarrow \eta\pi\pi} = 0.166 \pm 0.01 \pm 0.008 \quad (5)$$

which is in agreement with the PDG value of  $0.19 \pm 0.07$  [8] and represents an appreciable improvement in precision.

The  $f_1(1420)$  has also been observed in the  $K^*(892)\bar{K}$  decay mode by this experiment [6] and hence its branching ratio to  $a_0(980)\pi$  and  $K^*(892)\bar{K}$  has been calculated taking into account the unseen decay modes and geometrical acceptance effects and gives

$$\frac{f_1(1420) \rightarrow a_0(980)\pi}{f_1(1420) \rightarrow K^*(892)\bar{K}} = 0.04 \pm 0.01 \pm 0.01. \quad (6)$$

Hence a small ( $\approx 4\%$ ) contribution for the  $a_0(980)\pi$  decay mode should have been found in the analysis of the  $K_S^0 K^\pm \pi^\mp$  channel. However, a contribution at this level would have been at the limit of sensitivity.

There is considerable uncertainty in the branching ratio of the  $a_0(980)$  [8]. Since the  $f_1(1285)$  is observed in both the  $K_S^0 K^\pm \pi^\mp$  and  $\eta\pi^+\pi^-$  channels decaying effectively 100% to  $a_0(980)\pi$  we can use this information to determine the branching ratio of the  $a_0(980)$  to be

$$\frac{a_0(980) \rightarrow K\bar{K}}{a_0(980) \rightarrow \eta\pi} = 0.166 \pm 0.01 \pm 0.02 \quad (7)$$

where the systematic error has been increased to take into account any possible non- $a_0(980)\pi$  decay of the  $f_1(1285)$ .

We have previously published a paper on the  $\rho^0\gamma$  final state [13] in which we showed that there was only evidence for the  $\eta'$  and  $f_1(1285)$ . Using the

increase of a factor of ten in statistics in this current paper we want to improve on the measurement of the  $f_1(1285)$  branching ratio and the upper limit for  $f_1(1420) \rightarrow \rho^0\gamma$ . In addition, we want to search for possible  $\phi\gamma$  decay modes of both resonances. The reaction

$$pp \rightarrow p_f(h^+h^-\gamma)p_s \quad (8)$$

has been isolated from the sample of events having four outgoing charged tracks plus one  $\gamma$  with energy greater than 2.0 GeV reconstructed in the electromagnetic calorimeter by first imposing the following cuts on the components of the missing momentum:  $|\text{missing } P_x| < 12.0$  GeV/c,  $|\text{missing } P_y| < 0.10$  GeV/c and  $|\text{missing } P_z| < 0.06$  GeV/c. For the  $K^+K^-\gamma$  channel one of the central particles is required to be identified as being a  $K$  by the Čerenkov system and the other particle is required to be compatible with being a  $K$ . Energy balance is then used to select out the  $\pi^+\pi^-\gamma$  and  $K^+K^-\gamma$  channels. The major backgrounds to these channels come from the more copiously produced  $\pi^+\pi^-\pi^0$  and  $K^+K^-\pi^0$  channels where one of the  $\gamma$ s from the decay of the  $\pi^0$  is not detected and the resulting event passes through the momentum balance cuts. The contribution of this background to the selected channels has been simulated taking real  $\pi^+\pi^-\pi^0$  and  $K^+K^-\pi^0$  events and distributing them according to a Gaussian in Feynman  $x$  ( $x_F$ ) centered at  $x_F = 0$  in which the  $\pi^0$  has been allowed to decay isotropically.

Fig. 3(a) shows the selected  $\pi^+\pi^-\gamma$  mass spectrum together with the expected background from the  $\pi^+\pi^-\pi^0$  channel. Fig. 3(b) shows the resulting background subtracted  $\pi^+\pi^-\gamma$  mass spectrum where evidence can be seen for the  $\eta$ ,  $\eta'$  and  $f_1(1285)$ . Fig. 3(c) shows the  $\pi^+\pi^-$  mass spectrum from the selected  $\pi^+\pi^-\gamma$  events with the expected background from the  $\pi^+\pi^-\pi^0$  channel and Fig. 3(d) shows the resulting background subtracted mass spectrum which shows a threshold enhancement due to the  $\eta \rightarrow \pi^+\pi^-\gamma$  and a signal which has been identified as the  $\rho^0(770)$ . The  $\rho^0\gamma$  channel has been selected by requiring  $0.70 < m(\pi^+\pi^-) < 0.84$  GeV. Fig. 3(e) shows the  $\rho^0\gamma$  mass spectrum from the selected  $\pi^+\pi^-\gamma$  events with the expected background from the  $\pi^+\pi^-\pi^0$  channel and Fig. 3(f) shows the resulting background subtracted mass

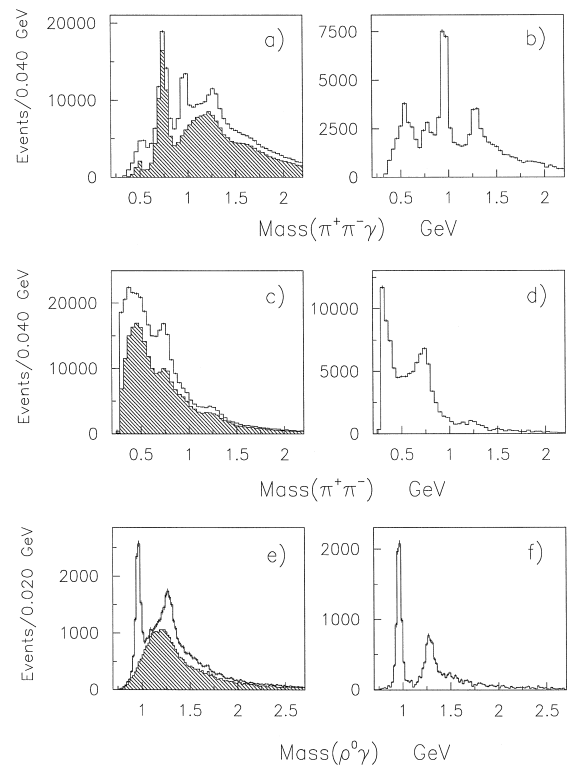


Fig. 3. (a) The  $\pi^+\pi^-\gamma$  mass spectrum with shaded the background from the  $\pi^+\pi^-\pi^0$  channel (b) the background subtracted  $\pi^+\pi^-\gamma$  mass spectrum. (c) The  $\pi^+\pi^-$  mass spectrum with shaded the background from the  $\pi^+\pi^-\pi^0$  channel (d) the background subtracted  $\pi^+\pi^-$  mass spectrum. (e) The  $\rho^0\gamma$  mass spectrum with shaded the background from the  $\pi^+\pi^-\pi^0$  channel (f) the background subtracted  $\rho^0\gamma$  mass spectrum.

spectrum which shows clear  $\eta'$  and  $f_1(1285)$  signals. There is no evidence for any signal in the 1.4 GeV mass region.

After acceptance correcting the data and taking into account the unseen decay modes we have determined the branching ratios of the  $\eta'$  and  $f_1(1285)$  to be

$$\frac{\eta' \rightarrow \rho^0\gamma}{\eta' \rightarrow \eta\pi\pi} = 0.43 \pm 0.02 \pm 0.02 \quad (9)$$

and

$$\frac{f_1(1285) \rightarrow \rho^0\gamma}{f_1(1285) \rightarrow \eta\pi\pi} = 0.10 \pm 0.01 \pm 0.02 \quad (10)$$

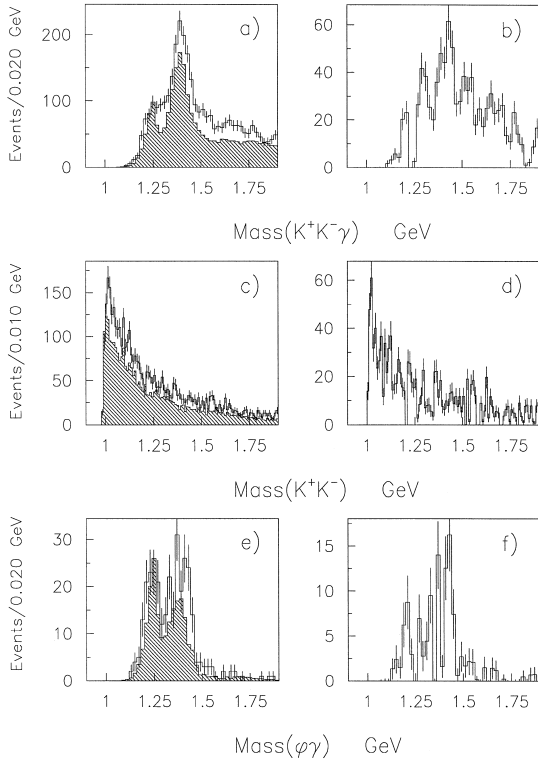


Fig. 4. (a) The  $K^+K^-\gamma$  mass spectrum with shaded the background from the  $K^+K^-\pi^0$  channel (b) the background subtracted  $K^+K^-\gamma$  mass spectrum. (c) The  $K^+K^-$  mass spectrum with shaded the background from the  $K^+K^-\pi^0$  channel (d) the background subtracted  $K^+K^-$  mass spectrum. (e) The  $\phi\gamma$  mass spectrum with shaded the background from the  $K^+K^-\pi^0$  channel (f) the background subtracted  $\phi\gamma$  mass spectrum.

both of which are in good agreement with the PDG values of  $0.459 \pm 0.025$  and  $0.108 \pm 0.046$  respectively [8].

For the  $f_1(1420)$  an upper limit has been calculated to be

$$\frac{f_1(1420) \rightarrow \rho^0\gamma}{f_1(1420) \rightarrow K\bar{K}\pi} < 0.02 \text{ (95\% c.l.)}. \quad (11)$$

This is an improvement on our previous upper limit of  $< 0.08$  [13].

For the  $\phi\gamma$  channel there is an additional problem in that the signals that we wish to study, namely the  $f_1(1285)$  and the  $f_1(1420)$ , are also present in the background  $K^+K^-\pi^0$  channel. However, since the method of background subtraction has been successful for the  $\pi^+\pi^-\gamma$  channel the same method will be

employed here. Fig. 4(a) shows the selected  $K^+K^-\gamma$  mass spectrum together with the expected background from the  $K^+K^-\pi^0$  channel. Fig. 4(b) shows the resulting background subtracted  $K^+K^-\gamma$  mass spectrum. Fig. 4(c) shows the  $K^+K^-$  mass spectrum from the selected  $K^+K^-\gamma$  events with the expected background from the  $K^+K^-\pi^0$  channel and Fig. 4(d) shows the resulting background subtracted mass spectrum which shows evidence for a  $\phi$  signal. The  $\phi\gamma$  channel has been selected by requiring  $1.01 < m(K^+K^-) < 1.03$  GeV. Fig. 4(e) shows the  $\phi\gamma$  mass spectrum from the selected  $K^+K^-\gamma$  events with the expected background from the  $K^+K^-\pi^0$  channel and Fig. 4(f) shows the resulting background subtracted mass spectrum which shows a possible excess of events in the  $f_1(1420)$  region.

If the events in the 1.42 GeV mass region are interpreted as being due to the  $f_1(1420)$  then after acceptance correcting the data and taking into account the unseen decay modes we have determined the branching ratio of the  $f_1(1420)$  to be

$$\frac{f_1(1420) \rightarrow \phi\gamma}{f_1(1420) \rightarrow K\bar{K}\pi} = 0.003 \pm 0.001 \pm 0.001. \quad (12)$$

For the  $f_1(1285)$  we can only calculate an upper limit of

$$\frac{f_1(1285) \rightarrow \phi\gamma}{f_1(1285) \rightarrow K\bar{K}\pi} < 0.005 \text{ (95\% c.l.)}. \quad (13)$$

The number obtained for the  $f_1(1285)$  is compatible with the PDG value of  $0.0082 \pm 0.0033 \pm 0.0020$ . A value for the  $f_1(1420)$  has not previously been measured.

Assuming that the only decay modes of the  $f_1(1285)$  are  $\pi\pi\pi\pi$ ,  $K\bar{K}\pi$ ,  $\eta\pi\pi$ ,  $\rho^0\gamma$  and  $\phi\gamma$  we have determined the branching fractions of the  $f_1(1285)$  as shown in Table 1. These values are

Table 1

The branching fractions of the  $f_1(1285)$

Decay mode	Fraction (%)
$\pi\pi\pi\pi$	$33.0 \pm 1.5 \pm 1.5$
$K\bar{K}\pi$	$8.7 \pm 0.4 \pm 0.4$
$\eta\pi\pi$	$52.8 \pm 3.8 \pm 2.5$
$\rho^0\gamma$	$5.4 \pm 0.4 \pm 0.3$
$\phi\gamma$	$< 0.043$ (95% c.l.)

compatible with those found in the PDG [8] but represent an increase in precision. Assuming that the only decay modes of the  $f_1(1420)$  are  $K^*(892)\bar{K}$ ,  $a_0(980)\pi$  and  $\phi\gamma$  we have determined the branching fractions of the  $f_1(1420)$  as shown in Table 2.

We have previously published the  $dP_T$  dependence, where  $dP_T$  is the difference in the transverse momentum vectors of the two exchange particles [5,14], of the  $f_1(1285)$  [6,7] and  $f_1(1420)$  [6]. However, due to an improved understanding and simulation of the experimental trigger, these values have now changed from the previously published values [6,7]. The fraction of  $f_1(1285)$  and  $f_1(1420)$  has been calculated for  $dP_T \leq 0.2$  GeV,  $0.2 \leq dP_T \leq 0.5$  GeV and  $dP_T \geq 0.5$  GeV and gives  $0.03 \pm 0.01$ ,  $0.35 \pm 0.02$  and  $0.61 \pm 0.04$  for the  $f_1(1285)$  and  $0.02 \pm 0.02$ ,  $0.38 \pm 0.02$  and  $0.60 \pm 0.04$  for the  $f_1(1420)$ . This results in a ratio of production at small  $dP_T$  to large  $dP_T$  of  $0.05 \pm 0.016$  for the  $f_1(1285)$  and  $0.03 \pm 0.03$  for the  $f_1(1420)$ . These ratios are similar to those found for other  $q\bar{q}$  mesons [15].

In order to determine the four momentum transfer dependence ( $t$ ) of the  $f_1(1285)$  and  $f_1(1420)$  the  $\eta\pi^+\pi^-$  and  $K_S^0 K^\pm \pi^\mp$  mass spectrum have been fitted in  $0.1 \text{ GeV}^2$  bins of  $t$ . Fig. 5(a) and (b) show the four momentum transfer from one of the proton vertices for the  $f_1(1285)$  and  $f_1(1420)$  respectively. The distributions have been fitted with a single exponential of the form  $\exp(-b|t|)$  and yields  $b = 6.3 \pm 0.3 \text{ GeV}^{-2}$  for the  $f_1(1285)$  and  $5.6 \pm 0.5 \text{ GeV}^{-2}$  for the  $f_1(1420)$ . These values are consistent with what is expected from Double Pomeron Exchange (DPE) [16].

The azimuthal angle ( $\phi$ ) is defined as the angle between the  $p_T$  vectors of the two protons. The  $\phi$  dependence of the  $f_1(1285)$  and  $f_1(1420)$  has been determined by fitting the  $\eta\pi^+\pi^-$  and  $K_S^0 K^\pm \pi^\mp$  mass spectrum in 20 degree bins in  $\phi$ . The resulting

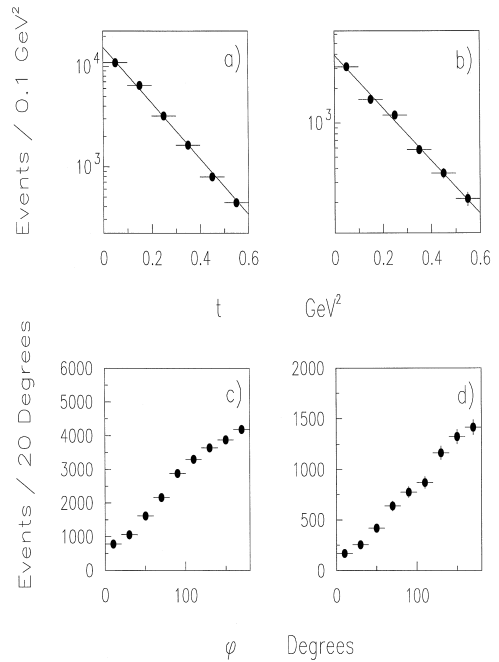


Fig. 5. The four momentum transfer squared ( $|t|$ ) from one of the proton vertices for (a) the  $f_1(1285)$  and (b) the  $f_1(1420)$ . The azimuthal angle ( $\phi$ ) between the two outgoing protons for (c) the  $f_1(1285)$  and (d) the  $f_1(1420)$ .

distributions are shown in Fig. 5(c) and (d) for the  $f_1(1285)$  and  $f_1(1420)$  respectively. These distributions are compatible with each other but differ significantly from those observed for the  $\pi^0$ ,  $\eta$ ,  $\eta'$  [17],  $\omega$  [18] and the  $\phi\phi$  [19] and  $K^*(892)\bar{K}^*(892)$  [20] final states.

After correcting for geometrical acceptances, detector efficiencies, losses due to cuts, and unseen decay modes, the cross-section for  $f_1(1285)$  and  $f_1(1420)$  production at  $\sqrt{s} = 29.1$  GeV in the  $x_F$  interval  $|x_F| \leq 0.2$  is  $\sigma(f_1(1285)) = 6919 \pm 886$  nb and  $\sigma(f_1(1420)) = 1584 \pm 145$  nb. This can be compared with the cross-sections found in the same interval at  $\sqrt{s} = 12.7$  [2] which we have recalculated to be  $\sigma(f_1(1285)) = 6857 \pm 1306$  nb and  $\sigma(f_1(1420)) = 1080 \pm 385$  nb. The cross section as a function of energy for both the  $f_1(1285)$  and  $f_1(1420)$  is found to be consistent with being flat or rising slightly with centre of mass energy which is consistent with them being produced via DPE [16]. In a previous publication it had been observed [2]

Table 2

The branching fractions of the  $f_1(1420)$

Decay mode	Fraction (%)
$K^*(892)\bar{K}$	$96.0 \pm 1.0 \pm 1.0$
$a_0(980)\pi$	$4.0 \pm 1.0 \pm 1.0$
$\phi\gamma$	$0.3 \pm 0.12 \pm 0.2$

that the cross-section for the  $f_1(1285)$  decreased from  $\sqrt{s} = 12.7$  to  $23.8$  GeV. However, this was due to the fact that the experiment at  $\sqrt{s} = 23.8$  GeV was only sensitive to  $\phi$  angles less than  $90$  degrees and the acceptance program that had been used assumed a flat  $\phi$  distribution. Hence it underestimated the cross section.

In conclusion, central production is a clean process in which to study the properties of the  $f_1(1285)$  and  $f_1(1420)$  due to their strong production relative to  $J^{PC} = 0^{-+}$  states in the same mass region. The branching fractions of the  $f_1(1285)$  and  $f_1(1420)$  in all major decay modes have been determined with improved accuracy. Both the  $f_1(1285)$  and  $f_1(1420)$  are consistent with being produced by DPE.

### Acknowledgements

This work is supported, in part, by grants from the British Particle Physics and Astronomy Research Council, the British Royal Society, the Ministry of Education, Science, Sports and Culture of Japan (grants no. 04044159 and 07044098), the Programme International de Cooperation Scientifique

(grant no. 576) and the Russian Foundation for Basic Research (grants 96-15-96633 and 98-02-22032).

### References

- [1] T. Armstrong et al., Phys. Lett. B 146 (1984) 273.
- [2] T. Armstrong et al., Zeit. Phys. C 34 (1987) 23; Phys. Lett. B 221 (1989) 216; Zeit. Phys. C 56 (1992) 29.
- [3] T. Armstrong et al., Zeit. Phys. C 52 (1991) 389.
- [4] M.C. Berisso et al., A.I.P. Conf. Proc. 432 (1997) 36.
- [5] D. Barberis et al., Phys. Lett. B 397 (1997) 339.
- [6] D. Barberis et al., Phys. Lett. B 413 (1997) 225.
- [7] D. Barberis et al., Phys. Lett. B 413 (1997) 217.
- [8] Particle Data Group, European Physical Journal C 3 (1998) 1.
- [9] S. Abatzis et al., Phys. Lett. B 324 (1994) 509.
- [10] B.S. Zou, D.V. Bugg, Phys. Rev. D 48 (1993) R3948.
- [11] F. James, M. Roos, MINUIT Computer Physics Communications 10 (1975) 343; CERN-D506, 1989.
- [12] S.U. Chung et al., Ann. d. Physik. 4 (1995) 404.
- [13] T. Armstrong et al., Zeit. Phys. C 54 (1992) 371.
- [14] F.E. Close, A. Kirk, Phys. Lett. B 397 (1997) 333.
- [15] A. Kirk, hep-ex/9803024.
- [16] S.N. Ganguli, D.P. Roy, Phys. Rep. 67 (1980) 203.
- [17] D. Barberis et al., Phys. Lett. B 427 (1998) 398.
- [18] D. Barberis et al., Phys. Lett. B 422 (1998) 399.
- [19] D. Barberis et al., Phys. Lett. B 432 (1998) 436.
- [20] D. Barberis et al., hep-ex/9807021.